14 (2022) 100148

Contents lists available at ScienceDirect

International Journal of Thermofluids

journal homepage: www.sciencedirect.com/journal/international-journal-of-thermofluids

# Influence of hot corrosion on pulsed current gas tungsten arc weldment of aerospace-grade 80A alloy exposed to high temperature aggressive environment

P. Subramani [a], N. Arivazhagan [b], Senthil Kumaran Selvaraj [b], Simone Mancin [c], M. Manikandan [b,*]

[a] Department of Mechanical Engineering, Faculty of Engineering and Technology – Jain University, Bangalore, 562 112, India
[b] School of Mechanical Engineering, Vellore Institute of Technology, Vellore, 632014, India
[c] Department of Management and Engineering, University of Padova, Vicenza, 36100, Italy

ARTICLE INFO

*Keywords:*
Alloy 80A
Hot corrosion
Oxidation
Molten salt
Pulsed current gas tungsten arc welding
Weldment
Substrate

ABSTRACT

One of the significant issues that shorten the life of components used in high-temperature applications is hot corrosion. The current study compares the performance of welded aerospace-grade 80A fabricated through continuous and pulsed gas tungsten arc welding techniques. Weld coupons are produced using two different filler wires (ERNiCrMo-3 (Mo-3) and ERNiCr-3 (Cr-3)). Welded substrates are subjected to 50 cycles of air oxidation and $Na_2SO_4$ + 60%$V_2O_5$ molten salt environmental conditions at 900 °C. Corrosion products were analysed through scanning electron microscope/energy dispersive spectroscopy and X-ray diffraction analyses. Thermogravimetric analysis revealed that all welded substrates trailed the parabolic rate of law kinetics. In the molten salt (MS) environment, gas tungsten arc welded (GTAW) Mo-3 substrate showed more weight gain. In contrast, a minor weight gain was observed in the pulsed current gas tungsten arc welded (PCGTAW) Cr-3 substrate. It indicates that accelerated corrosion kinetics was observed in the molten salt environmental condition that showed more weight gain than air oxidation. amongst the weldments, pulsed current gas tungsten witnessed superior corrosion-resistant behaviour. This phenomenon is observed due to grain refinement suppression of heat-affected zones and secondary phases in the weld fusion zone. In addition, the appearance of protective oxides such as $Cr_2O_3$, NbO and $NiCr_2O_4$ helps arrest the oxidation at the surface and sub-surface layer by providing good resistance against hot corrosion to the welded substrate. Thus, utilizing the PCGTAW technique during the fabrication/refurbishing process helps promote the material's corrosion resistance against a hot corrosion environment.

## Introduction

As described in thorough reviews, one of the methods to reduce energy usage is by recovering, reclaiming, or reusing waste heat generated [1,2,3]. The reclamation of heat is a particular area of interest as it has been reported that 70% of global energy demand in the industrial sector is for heat or thermal processes. Therefore, high-temperature waste heat management calls for advanced materials, coatings, and manufacturing techniques to meet consumer demand. As described by Pandis [4]' a feasible waste heat recovery technology can be condensing economizers, condensing heat exchangers etc., exploiting the latent heat of the flue gases. However, corrosion issues related to the high content of SOx, NOx, Cl etc., in the flue gases due to the formation of corrosive solutions such as $H_2SO_4$, HCl etc., after condensation, call for technical solutions with the improved corrosion resistance of the heat exchanging surfaces.

High-performance materials such as nickel-based superalloys were used for manufacturing, for example, the gas turbine component or heat exchangers [5]. Besides, the engine components are exposed to hazardous environments, where high temperature and high mechanical loading lead to fatigue cracks and damage due to foreign objects [6,7]. These damaged components are generally repaired/refurnished through welding to reduce the production cost of the new component. These engine components are also damaged due to the corrosive environment in the gas turbine [8,9]. The corrosion of components is due to a

* Corresponding author.
*E-mail address:* mano.manikandan@gmail.com (M. Manikandan).

https://doi.org/10.1016/j.ijft.2022.100148
Received 25 February 2022; Received in revised form 30 March 2022; Accepted 30 March 2022
Available online 1 April 2022

**Nomenclature**

| | |
|---|---|
| AO | Air Oxidation |
| MS | Molten Salt |
| GTAW | Gas Tungsten Arc Welding |
| PCGTAW | Pulsed Current Gas Tungsten Arc Welding |
| SEM | Scanning Electron Microscope |
| EDS | Energy Dispersive Spectroscopy |
| XRD | X-Ray Diffraction |
| ΔW | Change in Substrate Weight |
| A | Surface Area |
| Kp | Parabolic Rate Law Constant |
| t | Time |

combination of high temperature and the contaminants such as sulfur, sodium, and vanadium in the low-grade fuels used for operating the engine [9].

Hot corrosion is one of the significant problems that degrade the life of the components at high temperatures. Particularly at high-temperature molten salt (MS) ($Na_2SO_4$, $V_2O_5$, NaCl, etc.) environment conditions, the degradation of the components is exponentially increased [10]. In this research, alloy 80A welded substrates were open to air oxidation (AO) and MS environments at high temperatures. Alloy 80A is a precipitation strengthened nickel-based superalloy formed from the nickel-chromium system. This alloy is designed especially for an aeronautical application like gas turbine components (blade, ring, and disc) and is also used in Internal Combustion engines as an exhaust valve [11, 12].

The candidate material of this study is alloy 80A welded substrate used in high-temperature applications. When this substrate is exposed to high temperatures, component damage due to corrosion and erosion occurs, lowering the component's lifespan. These damaged components impact the machine's overall operation, resulting in time, money, and material losses. As such, many researchers have explored the corrosion behaviour of alloy 80A, which is susceptible to AO and MS conditions at high temperatures.

Kiamehr et al. [13] studied the hot corrosion demeanour of commercially available alloys such as alloy 153MA, alloy 214, alloy HR160, FeCrAlY, Nimonic 80A, and Kanthal APM. These commercial alloys were coated with potassium chloride (KCl) powder and then subjected to $N_2$ (g) + 15% $H_2O$ (g)+ 5% $O_2$ (g) (vol.%) gases environment at 600 °C for 168 hr. It is identified that the alloy 80A substrate exhibited more corrosion or material loss compared to other materials. The corroded alloy 80A substrate consists of the cavity depleted with Ti, Cr, Al and enriched in Ni. It is also identified that corrosion is rich in chromium phase ($Cr_{23}C_6$), titanium nitride (TiN), and aluminium.

In AO and MS conditions at 900 °C, Sreenivasulu and Manikandan [14] investigated the corrosion behaviour of thermal barrier coated and uncoated substrates. They discovered that an uncoated substrate coated with MS gained greater mass because the MS hastened the substrate's deterioration. The formation of $NiCr_2O_4$, $Cr_2O_3$, and NiO phases acts as the substrate protective barrier. Keienburg et al. [15] investigated the cause of failure of turbine blade made of alloy 80A. Author discovered that when alloy 80A turbine blades were subjected to high temperatures, continuous carbides film materialised in the interdendritic region, increasing the transition of MC type carbides to 22% coarsened γ' phase + 88% $M_{23}C_6$ (Cr rich precipitate) phase.

Cho et al. [16] explored the demeanour of superalloys (Inconel 713LC, Nimonic 90, and 80A alloys) in a high-temperature MS environment under oxidizing atmosphere. The alloys were subjected to 675 °C for 72 to 216 hr along with the substrate coated with MS LiCl–$Li_2O$. They found that the substrate of Nimonic 80A performed well compared to Nimonic 90 but was still inferior to alloy 713LC. They also indicated that the formation of $Li_2Ni_8O_{10}$ and $LiFeO_2$ phases deteriorated the substrate, and the development of (Cr, Ti)$_2O_3$ and $Cr_2O_3$ phases worked as a protective barrier by improving corrosion resistance.

In general, gas turbine components exposed to high-temperature applications are damaged due to corrosion/erosion or some external source or manufacture defects are usually refurbished or repaired through the welding process [16]. These refurbished or repaired components (through welding) are then exposed to the same hazardous environment as the defect-free component. These repaired/weld joints are severally attacked by corrosion because of the heterogeneity in the welded zone. From the literature, it can be seen that studies related to the hot corrosion behaviour of alloy 80A welded substrate is not studied. Thus this research work documents the effect of high temperature on the alloy 80A welded substrate that is open to AO and MS environment conditions. The results of this paper will be beneficial to the gas turbine manufacturing industries, understand the type of corrosion, the effect of high temperature-induced with MS environment on the substrate, and estimate the substrate's life.

## Materials and methodology

### *The substrate, filler metals, and working process*

Alloy 80A (chemical composition shown in Table 1) used in this study was procured in the plate form of 6 mm thickness. The alloy was machined using a wire electric W-EDM machine to the dimension of 5 × 50 × 170 mm and then cleaned with acetone to remove impurities on the material's surface before welding. V grooves were produced on alloy 80A and filled with ERNiCrMo-3 (Mo-3) and ERNiCr-3 (Cr-3) filler metals using gas tungsten arc welding (GTAW) and pulsed current gas tungsten arc welding (PCGTAW).

The process parameter used for achieving the defect-free welds were already stated in the published literature of the authors [17, 18]. The hot corrosion test substrates of size 20 × 15 × 6 mm were extracted from the welded substrates through WEDM. The above size of the substrate is determined so that substrate consists of FZ, HAZ and BM since in actual application, refurnished parts consists of all the three zones when exposed to a hot corrosion environment. The extracted substrates surface are then polished on all six sides using silicon carbide emery sheets to eliminate any imperfection. The irregularities on the substrate surface can induce and accelerate the corrosion on that specific spot. After completing the polishing, the substrate is then again cleaned with acetone to remove fine powders of the substrate resulting from emery polishing.

### *Hot corrosion test*

The performance of alloy 80 welded substrate fabricated with GTAW and PCGTAW procedure using ERNiCrMo-3 (Mo-3) and ERNiCr-3 (Cr-3) filler wires on AO and in MS environments at 900 °C under cyclic circumstances is investigated in this work. For molten salt environments, $Na_2SO_4$ + 60% $V_2O_5$ combined with distilled water and sprayed at a rate of 3 to 5 mg/cm$^2$ across the six sides of the welded substrate, both GTAW and PCGTAW (both Mo-3 and Cr-3). These MS-coated welded substrates are put in a box furnace at 200 °C for 3 h to eliminate moisture and for molten salt adherence to the welded substrates' surface. Before being exposed to a heat corrosion investigation, the weight of MS coated, and uncoated welded substrates are done using an electrical balance. These weighted welded are then exposed to a cyclic hot corrosion investigation at 900 °C, in which they are exposed to AO and MS conditions. The testing consists of heating at 900 °C for 1 hour and then 20 min cooling in a sand bath to reach room temperature (one cycle). Then, the same procedure was repeated for consecutive cycles up to 50 cycles. During this time, the substrates were weighed after each cycle to determine the weight increase in the substrate.

**Table 1**
Elemental composition (Wt.%) of the parent metal and filler wires.

| | Chemical composition (Wt.%) | | | | | | |
|---|---|---|---|---|---|---|---|
| | Ni | Cr | Fe | Al | Ti | Mn | Other |
| Substrate alloy 80A | Bal. | 20.43 | 0.052 | 1.58 | 2.47 | 0.358 | 2.0 (Co), 0.143 (Si), 0.072 (C), 0.010 (S), |
| Filler wire ERNiCrMo-3 | Bal. | 22.0 | 1.0 | 0.40 | 0.40 | 0.50 | 10.0 (Mo), 4.5 (Nb), 0.5 (Si), 0.5 (Cu), 0.1 (C), 0.015 (S) |
| Filler wire ERNiCr-3 | Bal. | 19.58 | 0.751 | 0.27 | 0.43 | 0.27 | 2.424 (Nb), 0.38 (Si), |

*Metallurgical characterization*

Macroscale examinations were conducted on hot corrosion exposed substrates for every 5 cycles up to the final 50th cycle. A scanning electron microscope (SEM) (Make: Carel Zeiss) was used to analyse the structural morphology. In addition, electron dispersive spectroscopy (EDS) (Make: Oxford instrument X-act) was performed on the welded substrates to analyse elements of corrosion products. Furthermore, X-ray diffraction (XRD) analysis was conducted on hot corrosion exposed MS applied substrate and uncoated substrate to identify the corrosion product.

## Results

*Visual examination*

The initial surface morphology of all the molten salt coated and uncoated substrates was captured with optical macroscopy before subjected to a hot corrosion test. After the exposure of substrates to the 1st cycle, the colour of the whole substrates was changed to grey colour for AO substrates and blackish-grey colour for the MS coated substrate. At the 2nd cycle, the weld zone of AO substrates started to change to black colour, and for coated substrates, the weld zone (WZ) turned dark black. At the 3rd cycle, the weld zone of all the AO substrates completely changed to black colour, and it maintained the same colour till the 50th cycle without any spallation. In the case of MS coated substrates, a layer of blackish powder was formed on the weld surface at the end of the 4th cycle. Spallation of weld zone surface occurs at the end of the 6th cycle in all MS coated PCGTAW, and it is found to increase slowly in the subsequent two-cycle. As for GTAW Cr-3 weld samples, spallation started at the 15th cycle, but in the case of the GTAW Mo-3 sample, white spots were observed at the 12th cycle, and spallation started at the 13th cycle. At the 10th cycle, the weld zone of PCGTAW Cr-3 substrate turned to a grey colour, and spallation started at the 15th cycle and gradually increased in the subsequent cycles. At the end of the 10th cycle, the weld zone of PCGTAW Mo-3 substrate started to change to a light green colour, and the spallation started at the 13th cycle and increased gradually in the subsequent cycles. The light greenish layer is started to form in the weld zone of the GTAW Mo-3 sample at the 16th cycle, and it gradually increased and formed a thick greenish layer at the end of the 38th cycle and remained the same till the 50th cycle. In PCGTAW Mo-3, the weld zone is completely covered with a greenish layer at the 18th cycle, and it forms a thick layer at the end of the 36th cycle, maintaining the same till the 50th cycle. As for the PCGTAW Cr-3 sample, complete spallation of the weld region is observed at the 43rd cycle, and it remained the same till the 50th cycle. Fig. 1 shows the 50th cycle surface morphology of both GTAW and PCGTAW welded substrate open to AO and MS environments.

*Corrosion kinetics*

Figs. 2 and 3 depict the weight change of the welded samples (in both AO and MS conditions) throughout 50 cycles. The graph (Fig. 2) indicates that AO substrates have a lower total weight increase than MS environment substrates. On the other hand, regardless of the welded substrates, MS environment welded substrates acquire more weight than AO substrates, which might be related to MS commencement and acceleration of corrosion on the welded substrates.

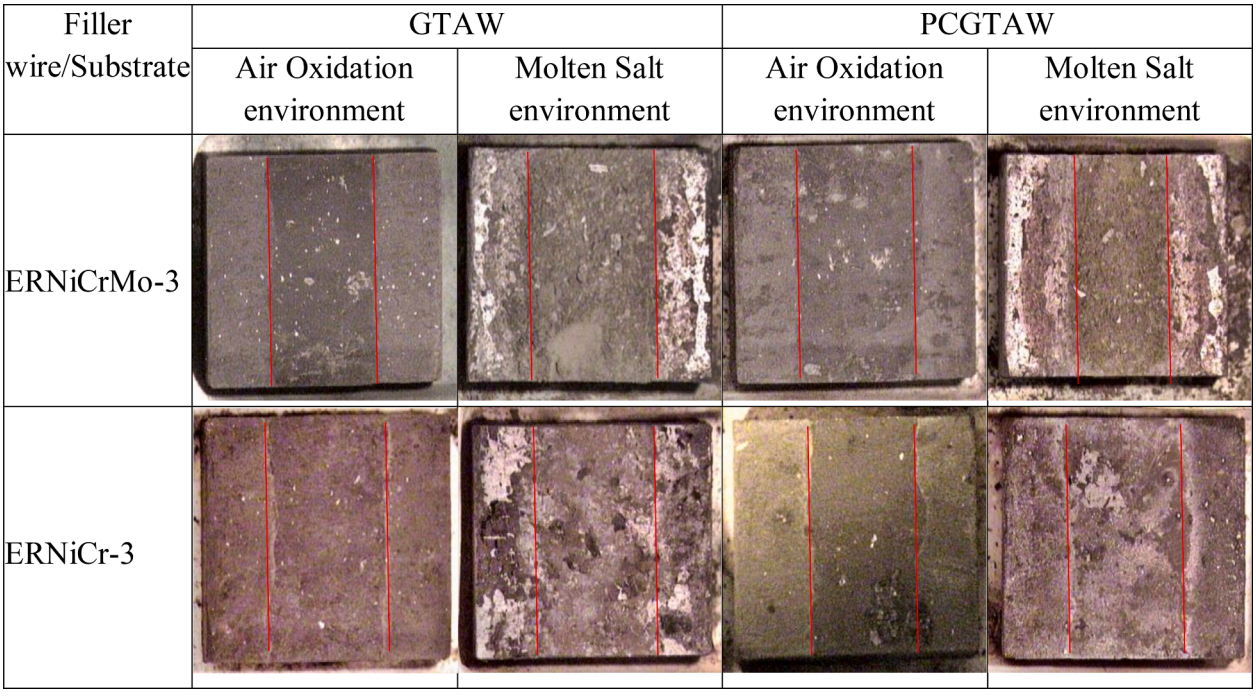


**Fig. 1.** 50th cycle surface morphology of both GTAW and PCGTAW welded substrate open to both AO and MS environment.

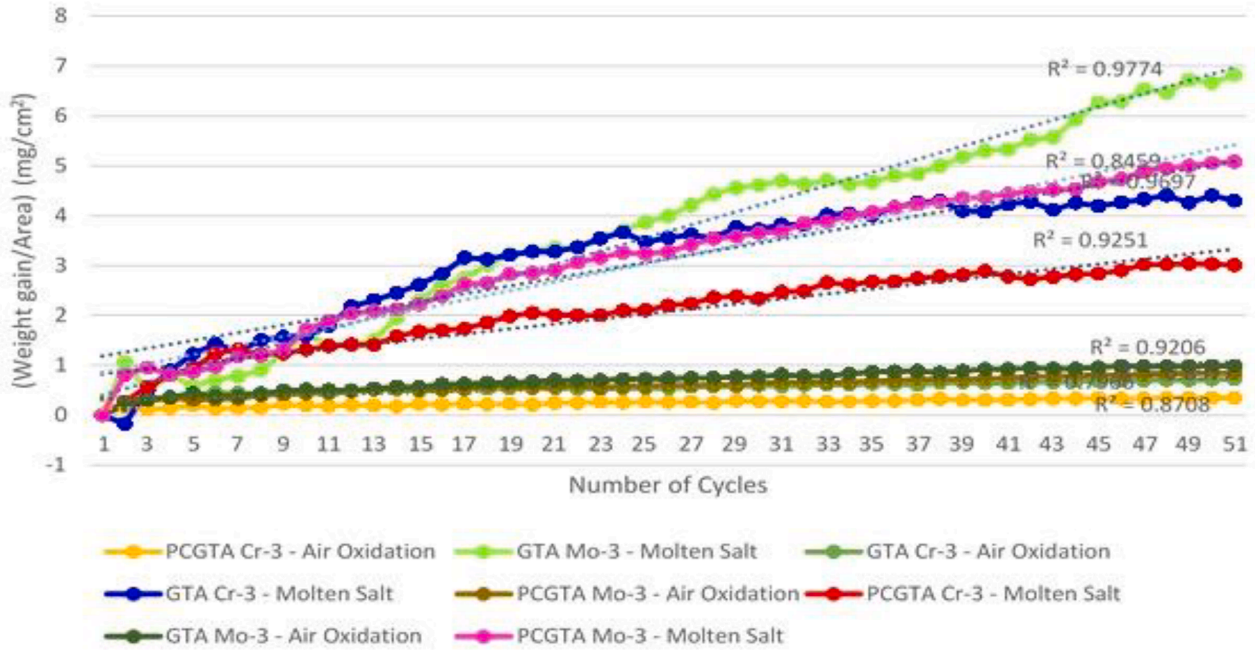


**Fig. 2.** Cumulative weight gain Vs number of cycles graph of welded sample that are subjected to both AO and MS environment.

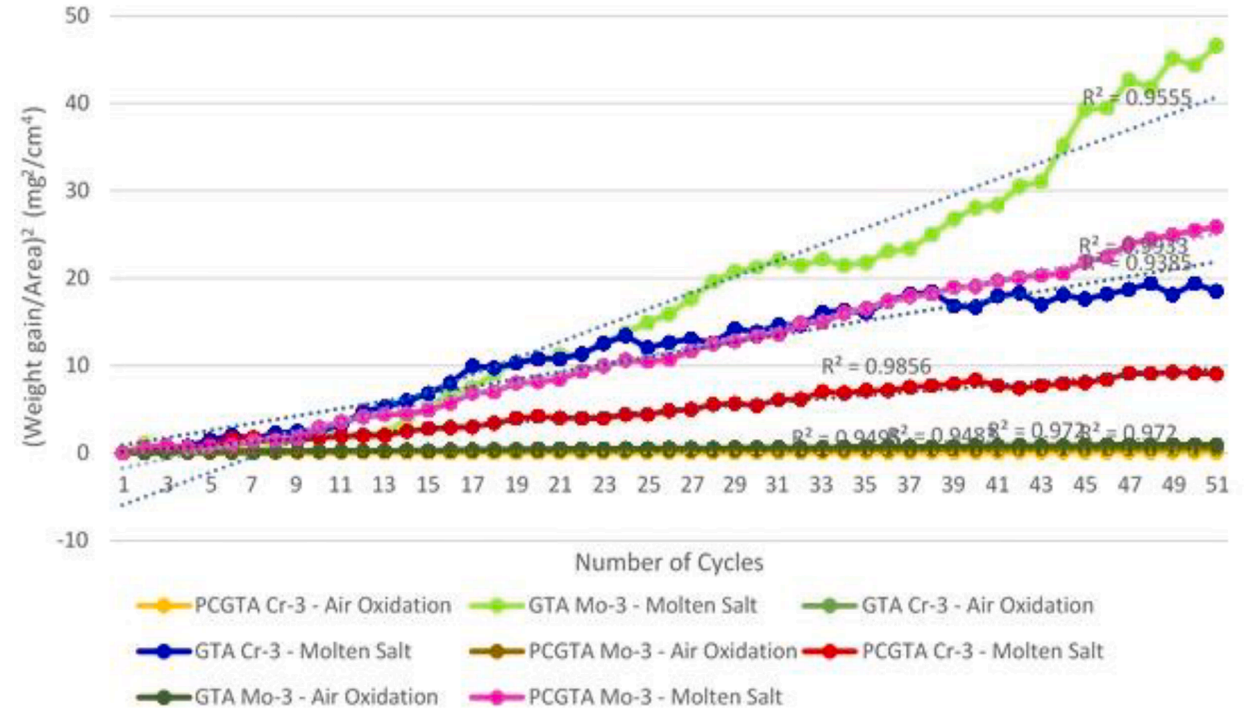


**Fig. 3.** Cumulative weight gain square Vs number of cycles graph of welded sample that are subjected to both AO and MS environment.

During the initial cycle period (1 to 4 cycles), a quick surge in weight for all the welded substrates due to rapid oxide formation such as Ni and Cr oxides on the surface of the welded substrates is found. Following the initial period of cycles, the weight of all substrates began to grow steadily. High weight gain was noted in GTAW Mo-3 substrate followed by GTAW Cr-3 substrate than its respective PCGTAW substrates. It indicates that GTAW welding is helpful for the occurrence of corrosion by accelerating oxide formation such as Fe, Na, Cr, V, S, and other harmful oxides. On the other hand, less weight gain was observed in the PCGTAW Cr-3 substrate followed by PCGTAW Mo-3 substrate than its respective GTAW substrates.

Furthermore, it indicates that the PCGTAW mode of welding is helpful in the development of more protective oxide layers such as Ni, Cr, Al, and other oxides than the GTAW substrates. Overall, from Fig. 2, it is inferred that PCGTAW welded substrates performed well compared to their respective GTAW welded substrates. It is also ascertained that PCGTAW Cr-3 substrate performed better than the PCGTAW Mo-3 substrate in an MS environment.

The parabolic rate (Kp) was determined using a linear least square Eq. (1),

$$(\Delta W|A)^2 = K_p \times t \quad (1)$$

Whereas A denotes the sample's surface area, t denotes time (s) and ΔW changes in substrate weight. The value of Kp ($g^2/cm^4/s^1$), total weight gain ($mg/cm^2$), total weight gain square $(mg/cm^2)^2$ of GTAW, and PCGTAW (both Mo-3 and Cr-3) substrates exposed to AO and MS conditions were shown in Table 2.

All welded substrates follow the parabolic route, as seen in Figs. 2 and 3. The rapid rise in weight observed in specific cycles is owing to the MS environment's faster synthesis of oxides (Fe, Na, Cr, V, S, and other hazardous oxide phases). The evaporation of Na and Cr volatile oxides at 900 °C from the substrates surface and sub-surface layer causes the sudden weight loss observed in specific cycles [19]. There is a steady drop in weight seen during the last stage of cyclic oxidation (40 to 50 cycle), which is related to the production of a protective oxide layer (Ni, Cr, Al, and other oxides) that prevents fast oxidation from the substrates surface and sub-surface layers.

*Surface analysis by SEM/EDS analysis*

The SEM/EDS examination is performed at a specific location on the welded substrates surface to detect the corrosion product or protective oxides triggered by air and MS at 900 °C. Fig. 4 shows SEM/EDS study on welded substrate surface produced through the GTAW and PCGTAW techniques using ERNiCrMo-3 filler wire.

Fig. 4 shows that both GTAW and PCGTAW Mo-3 welded substrates have identical significant elements such as O, Ni, Cr, and Ti, Mo, and minor elements such as Al, Nb, Fe, and Mn on the surface of the substrate in the AO environment (Figs. 4a and 4c). The significant elements in the MS environment (Figs. 4b and 4d) were discovered to be O, Ni, Cr, Nb, Mo, Na, and V, with minor elements being Al, Ti, Mn, Fe, and S. Fig. 5 depicts the 50th cycle SEM/EDS analysis of a welded substrate created utilizing GTAW and PCGTAW techniques with ERNiCr-3 (Cr-3) filler wire and subjected to AO and MS. In the case of GTAW and PCGTAW Cr-3 welded substrates in an AO environment (Figs. 5a and 5c), the major elements were O, Ni, Cr, and Nb, while minor elements included Al, Ti, Fe, and Mn. In the MS environment (Figs. 5b and 5d), the dominant elements were O, Ni, Cr, Nb, Ti, Na, and V, with Al, Fe, Mn, and S as minor elements.

*XRD analysis*

XRD analysis is performed in the centre of the welded component to detect the protective oxide phases and the corrosion product phases that arise from hot corrosion caused by both AO and MS conditions. XRD study of GTAW and PCGTAW welded substrates (ERNiCrMo-3) subjected to AO and MS conditions is shown in Fig. 6. It is evident from the results that both GTAW and PCGTAW Mo-3 AO substrates have prominent phases such as $Cr_2O_3$, $TiO_2$, and other minor phases are found to be NiO, $NiCr_2O_4$, $MoO_3$, $Al_2O_3$, $MnO_2$. In the case of MS substrates, prominent phases were $Cr_2O_3$, $TiO_2$, $MoO_3$, $NiCr_2O_4$, NbO, $NaVO_3$, and minor phases were $Al_2O_3$, $MnO_2$, NiO, $Fe_2O_3$, and $Cr_2S_3$.

Fig. 7 shows the XRD analysis of GTAW and PCGTAW welded substrates (ERNiCr-3) exposed to AO and MS environments. In AO substrate (both GTAW and PCGTAW), the prominent phase is protective $Cr_2O_3$, $NiCr_2O_4$, and NbO oxides and the minor phases are found to be $Al_2O_3$, $TiO_2$, $MnO_2$, NiO, $Fe_2O_3$. In the case of MS substrate, the prominent phase is found to be $Cr_2O_3$, $NiCr_2O_4$, $NaVO_3$, $TiO_2$, NbO, and the minor phases are $Al_2O_3$, $MnO_2$, NiO, $Fe_2O_3$ and $Cr_2S_3$. Table 3 also shows the prominent and minor phases of all the welded substrates for better understanding.

**Table 2**
Parabolic rate law constants of both GTA and PCGTA substrates (Mo-3 and Cr-3) exposed to AO and MS conditions at 900 °C.

| Filler Wire | Weld/ Environment | Total Weight Gain (mg/ $cm^2$) | Total Weight Gain Square $(mg/cm^2)^2$ | Parabolic Rate Law Constant (Kp) ($g^2/cm^4/s^1$) |
|---|---|---|---|---|
| ERNiCrMo-3 | GTAW – Air Oxidation | 0.991 | 0.982 | $5.18\times10-6$ |
| | GTAW – Molten salt | 6.821 | 46.595 | $2.53 \times 10^{-4}$ |
| | PCGTAW – Air Oxidation | 0.848 | 0.719 | $3.74 \times 10^{-6}$ |
| | PCGTAW – Molten salt | 5.084 | 25.856 | $1.4 \times 10^{-4}$ |
| ERNiCr-3 | GTAW – Air Oxidation | 0.725 | 0.526 | $2.57 \times 10^{-6}$ |
| | GTAW – Molten salt | 4.302 | 18.505 | $1.03 \times 10^{-4}$ |
| | PCGTAW – Air Oxidation | 0.345 | 0.118 | $5.16 \times 10^{-7}$ |
| | PCGTAW – Molten salt | 3.009 | 9.054 | $4.99 \times 10^{-5}$ |

## Discussion

The current study investigates the performance of alloy 80A weldments created using the GTAW and PCGTAW welding procedure using ERNiCrMo-3 and ERNiCr-3 filler wire in hot corrosion induced by AO and MS conditions at 900 °C. Fig. 1 shows that welded substrates in an AO environment have less corrosion than welded substrates in a non-AO environment. Due to the onset and acceleration of corrosion generated by the MS, high corrosion has been observed in the MS environment welded substrates [10]. Figs. 2 and 3 show that welded substrates gained much weight during the early stages of the cycles (upto the 4th cycle). After that, there is a gradual increase in the weight irrespective of the difference in the welded substrates. This phenomenon can be observed in the visual examination by way of change in colour of the welded substrate from its initial metallic colour to grey colour and followed by blackish-grey colour at the initial cycle period and then changed to complete black or gradually turning to greenish colour during the later period of cycles (5th to 50th cycles). This high weight gain exhibited at the initial cycles (up to 4th cycle) by the welded substrate is due to rapid oxidation, i.e. formation of oxides taking place at the welded substrates surface subjected to hot corrosion [19]. The formation of $Cr_2O_3$ oxides on the substrate's top surface layer acts as a diffusion barrier, preventing oxide from diffusing into the substrate's subsurface layer. As a result, only a small amount of oxide forms on the substrate, eventually leading to a constant oxidation state in the AO substrate [20]. Thus, it is evident from TGA results that AO substrates followed the parabolic path [20].

Performance/resistance of welded substrate (Mo-3 and Cr-3) against hot corrosion in AO environment at 900 °C is arranged as follows (Figs. 2 and 3)

PCGTAW Cr-3 > GTAW Cr-3 > PCGTAW Mo-3 > GTAW Mo-3

It is evident from Table 2 that the PCGTAW substrate showed better corrosion resistance than the GTAW substrate in the AO environment at 900 °C. This might be owing to the weld's grain refinement, which led to the creation of additional surface protective oxides, such as $NiCr_2O_4$, $Cr_2O_3$, $Al_2O_3$, and NbO, which leads to high corrosion resistance [21]. The corrosion resistance of PCGTAW Cr-3 substrate was higher than that of PCGTAW Mo-3 substrate, which might be related to the development of more $Cr_2O_3$, NbO, and NiCr2O4 oxides at the substrate's surface as a result of weld grain refinement. The EDS and XRD examination (Figs. 5c and 7c) demonstrate that NbO is found in low-intensity peaks, whereas Cr is found in two higher-intensity peaks, indicating the creation of $Cr_2O_3$. The grain refinement calculation for the weldments can be inferred from previously published articles by the author [17, 18]. In the case of PCGTAW Mo-3 substrate, the simultaneous presence of protective and non-protective oxides such as NbO, $Al_2O_3$, $Cr_2O_3$, $MoO_3$, $Fe_2O_3$ and $MnO_2$ are formed due to grain refinement are seen minor peaks that tend to increase the weight of the substrate slight higher than the GTAW Cr-3 substrates.

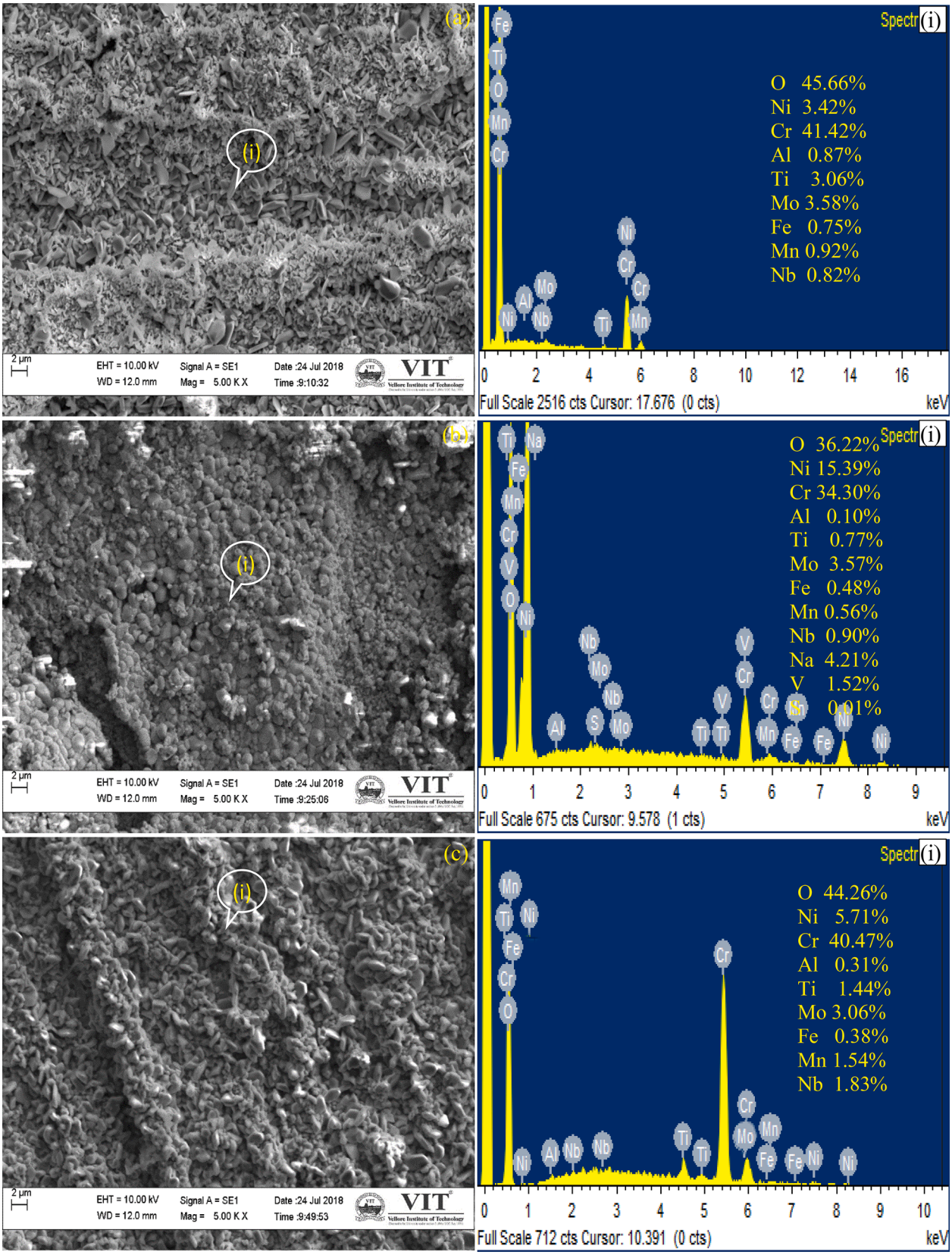


**Fig. 4.** 50th cycle SEM/EDS analysis of alloy 80A welded with ERNiCrMo-3 filler wire (a) GTAW- air oxidation (b) GTAW - molten salt; (c) PCGTAW - air oxidation and (d) PCGTAW - molten salt.

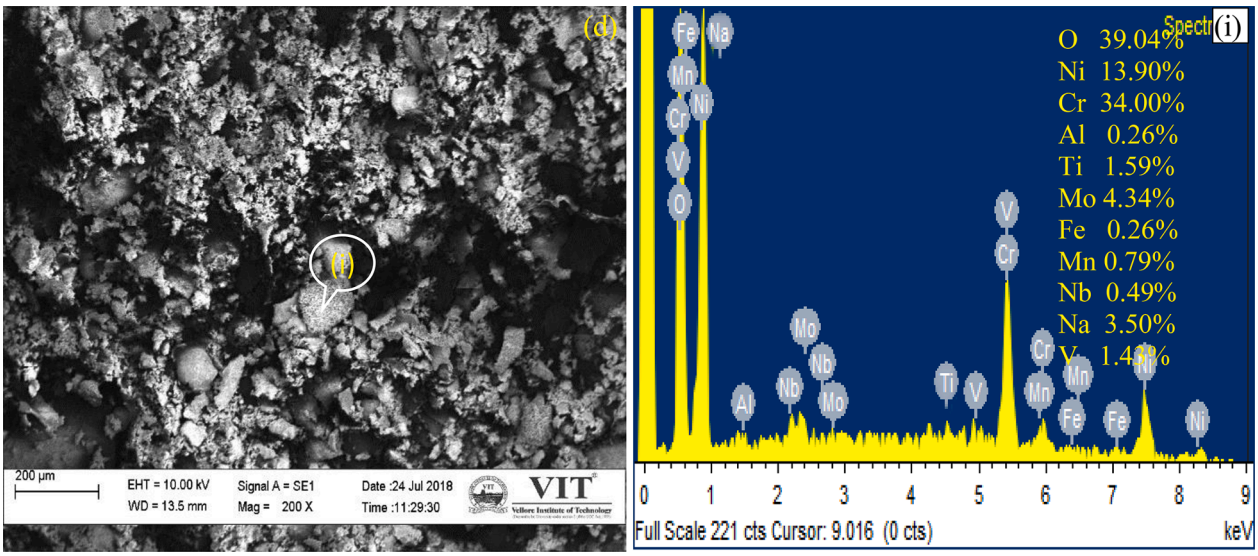


**Fig. 4.** (*continued*).

In GTAW Cr-3 and GTAW Mo-3 substrate, the corrosion resistance is provided by protective oxides such as $Cr_2O_3$, $Al_2O_3$ and NbO. However, from EDS analysis (Figs. 5a and 4a), it is seen that the Nb element is slightly higher in GTAW Cr-3 substrate, which might attribute to the form more of NbO oxide. The presence of NbO and the absence of non-protective $MoO_3$ oxide leads to the better corrosion resistance of the GTAW Cr-3 substrate than the PCGTAW Mo-3 substrate. In the case of the GTAW Mo-3 substrate, the presence of Mo element mainly non-protective $MoO_3$ and other $Fe_2O_3$ and $MnO_2$ oxides, along with the absence of grain refinement and protective NbO oxide, tend to increase the weight of the substrate by providing least corrosion resistance than GTAW Cr-3 and other PCGTAW substrates.

In EDS analysis, the most significant elements in the MS environment substrate are O, Ni, and Cr. As a result, the kinetics of corrosion of these components with MS ($Na_2SO_4 + V_2O_5$) are explained. The results of TGA (Figs. 2 and 3) show that the MS substrates are attributed to rapid oxidation in the initial cycles. Active element oxides cause this behaviour in the welded substrate [22]. At 400 °C, some active elements, such as Ni, create NiO, while at 500 °C to 600 °C, $Cr_2O_3$ oxide forms.

$$Ni + O \rightarrow NiO \tag{1}$$

[23]

$$2Cr + \frac{3}{2}O_2 \rightarrow Cr_2O_3 \tag{2}$$

[23]

The NiO and $Cr_2O_3$ oxides in the MS substrate prevent oxygen from diffusing into the substrate's sub-surface layer. They are formed selectively at first, then steadily rise in following cycles to steady-state of oxidation at later cycles as the exposure duration progresses [24, 25]. The creation of $NaVO_3$ oxide, which has a melting point of 610 °C, may also be responsible for the quick rise in weight during initial cycles [25]. The reaction between $Na_2SO_4$ and $V_2O_5$ (MS) at 900 °C produces this $NaVO_3$ oxide.

$$Na_2SO_4 + V_2O_5 \rightarrow 2NaVO_3 + SO_2 + \frac{1}{2}O_2 \tag{3}$$

[25]

$NaVO_3$ oxide works as a catalyst and an O carrier during the early cycles, causing the substrate to be oxidised and protective oxides to develop [26]. Simultaneously, there might also be the dissolution of $Cr_2O_3$ oxide to form $Na_2CrO_4$ oxide due to its reaction with MS at high temperatures.

$$4NaVO_3 + Cr_2O_3 + \frac{3}{2}O_2 \rightarrow 2Na_2CrO_4 + 2\,V_2O_5 \tag{4}$$

[26]

When $NaVO_3$ oxide reacts with protective $Cr_2O_3$ scales, it dissolves the surface $Cr_2O_3$ scales and forms volatile $Na_2CrO_4$ oxides. These volatile $Na_2CrO_4$ oxides evaporate as a gas at 900 °C [26]. It produces a cavity in the protective $Cr_2O_3$ layered scales, which results in rapid oxidation by inward diffusion of oxygen to subsurface layers of the substrates. Simultaneous growth and dissolution of protective $Cr_2O_3$ scales in the substrate surface attributed to the increase in substrate weight at a later period of cycles after initial cycles [26]. Thus, from Figs. 2 and 3, it is evident that all the MS substrates seem to little deviate from parabolic rate law.

Performance/resistance of welded substrates (Mo-3 and Cr-3) against hot corrosion in MS environment at 900 °C is arranged as follows (Figs. 2 and 3)

PCGTAW Cr-3 > GTAW Cr-3 > PCGTAW Mo-3 > GTAW Mo-3

The above arrangement signifies the increase in resistance to hot corrosion from the left to the right side. It is also evident from Table 3 that PCGTAW substrates performed better when compared to their respective GTAW substrate. This might be due to the grain refinement achieved in the PCGTAW substrates. PCGTAW Mo-3 and Cr-3 substrate achieved 15.62% and 4.01% grain refinement in the weld zone compared to its respective GTAW substrates [17, 18]. The pulsating current produced during the welding of alloy 80A causes grain refinement in the WZ. The authors' prior published research explains the process of grain refining in the WZ owing to the PCGTAW approach [17, 18]. The presence of grain refinement in PCGTAW WZ indicates the presence of more grains and grain boundaries (dislocation planar) in the WZ. These dislocation planar offers routes for elements diffusion (such as Cr and Ni) from the sub-surface layer to the weld face [21].

By limiting further inward diffusion of oxides to the sub-surface of the weld, these dispersed elements react with oxygen to generate more protective oxides $Cr_2O_3$ and $NiCr_2O_4$ layers on the weld surface, minimising the weight increase of PCGTAW substrates compared to their respective GTAW substrates. In addition, the stronger affinity of Cr with $O_2$ creates $Cr_2O_3$ oxides, which stop additional oxygen potential and encourage NiO development [22, 24]. Choi et al. [27] found similar results in their research. In addition to binary oxides, they discovered that ternary oxides such as $NiCr_2O_4$ occur during the intermediate stages of hot corrosion.

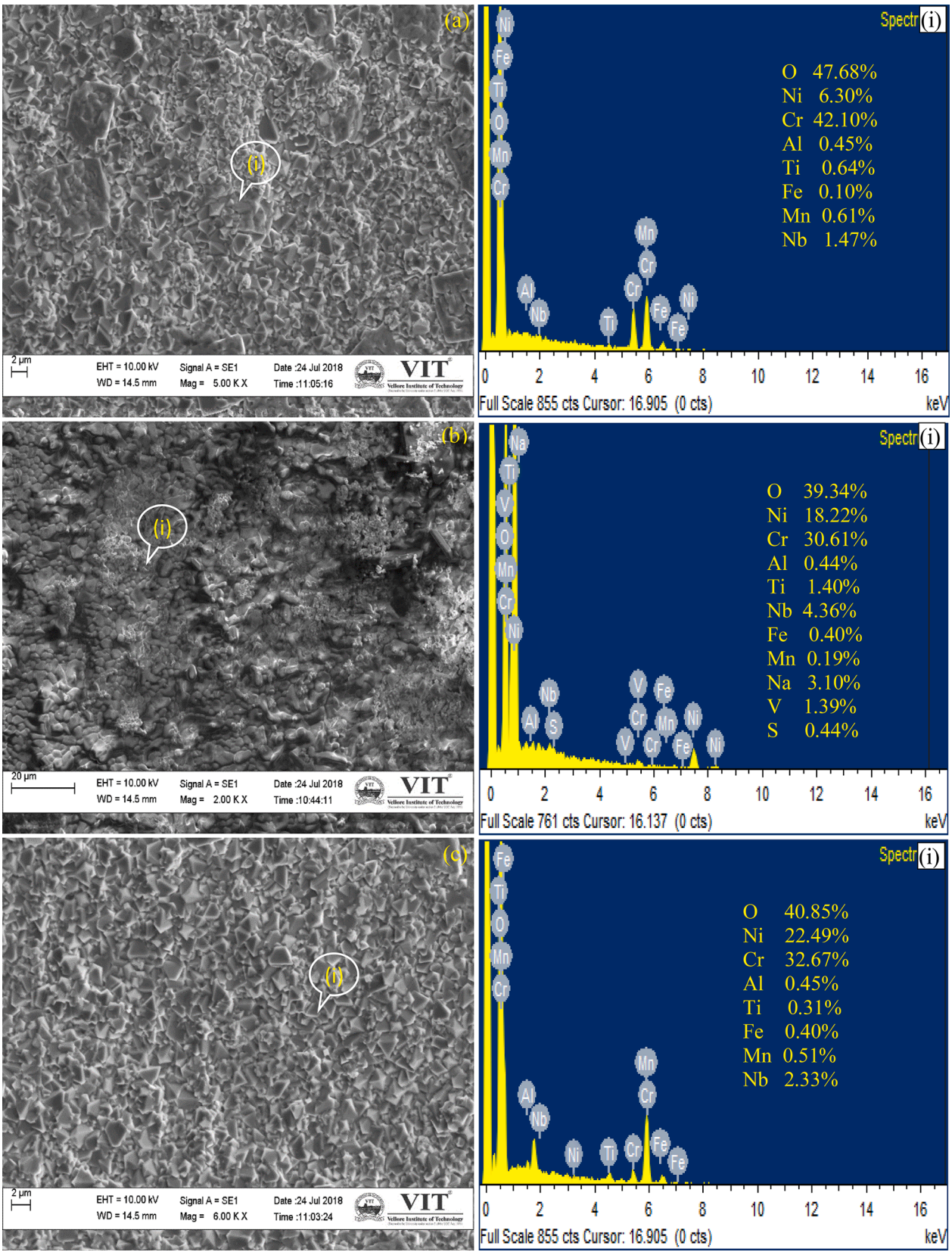


**Fig. 5.** 50th cycle SEM/EDS analysis of alloy 80A welded with ERNiCr-3 filler wire (a) GTAW- air oxidation (b) GTAW - molten salt; (c) PCGTAW - air oxidation and (d) PCGTAW - molten salt.

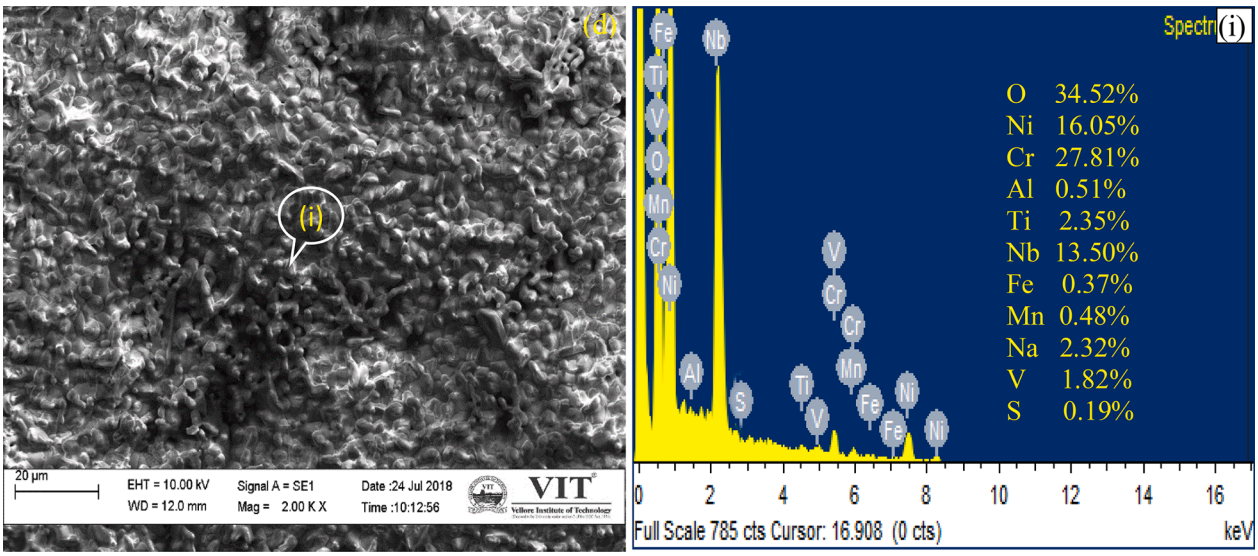


**Fig. 5.** (*continued*).

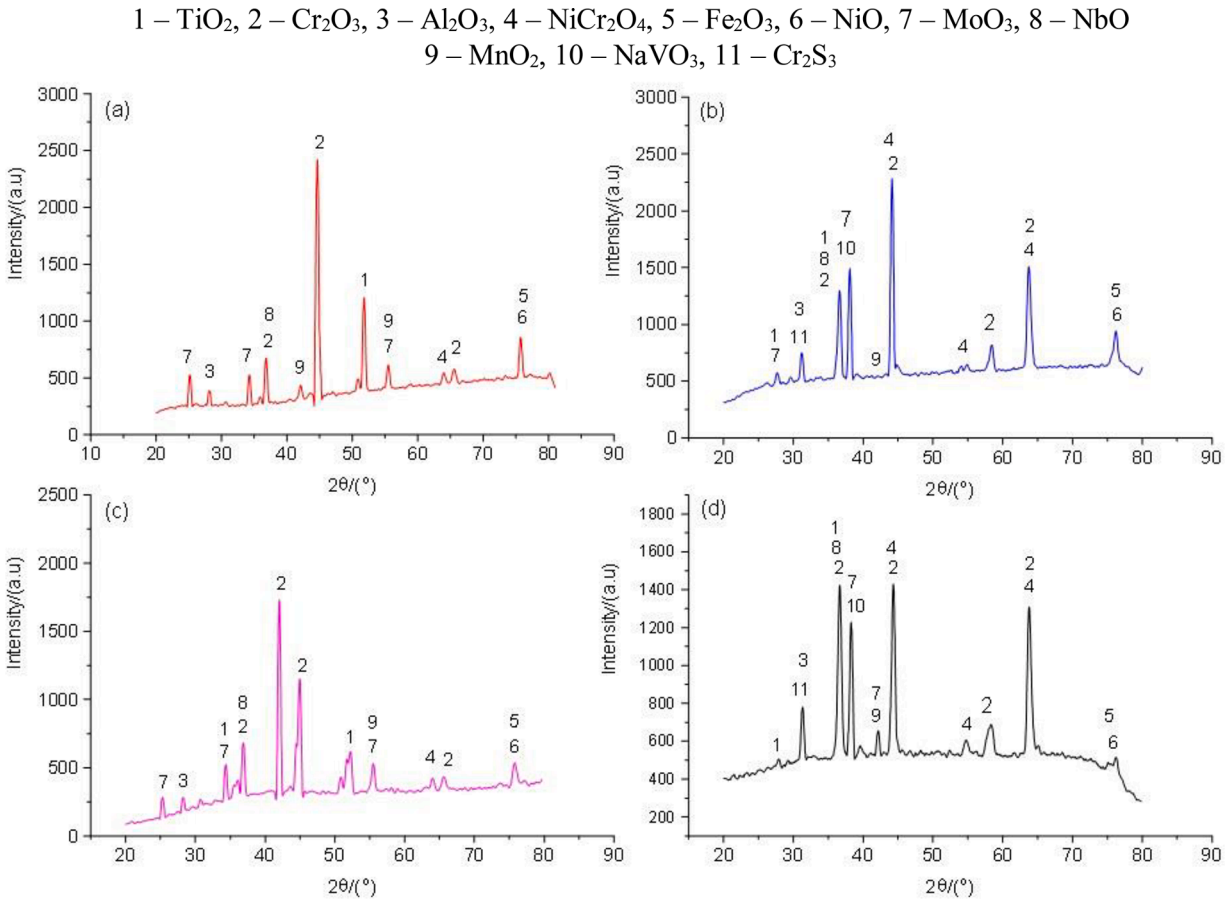


**Fig. 6.** XRD analysis of alloy 80A welded with ERNiCrMo-3 filler wire (a) GTAW- air oxidation (b) GTAW - molten salt; (c) PCGTAW - air oxidation and (d) PCGTAW - molten salt.

$$NiO + Cr_2O_3 \rightarrow NiCr_2O_4 \quad (5)$$

[27, 28]

Spinel $NiCr_2O_4$ oxide has a lower cation and anion transport coefficient than patent oxides; thus, the creation of spinel $NiCr_2O_4$ oxide on the substrate's surface raises oxidation resistance [20]. Figs. 2, 3, and Table 2 show that the PCGTAW Cr-3 substrate exhibits the least weight growth in the MS environment, which might be attributed to grain refinement in the substrate. Protective oxides $Cr_2O_3$, NbO, and $NiCr_2O_4$ develop on the substrate surface due to grain refinement. Furthermore, it stops oxygen from diffusing inside, reducing weight growth compared to other substrates. The results of XRD analysis match with EDS results as more Ni, Cr and Nb precipitations are observed on the substrate.

The GTAW Cr-3 substrate showed less weight than the PCGTAW Mo-

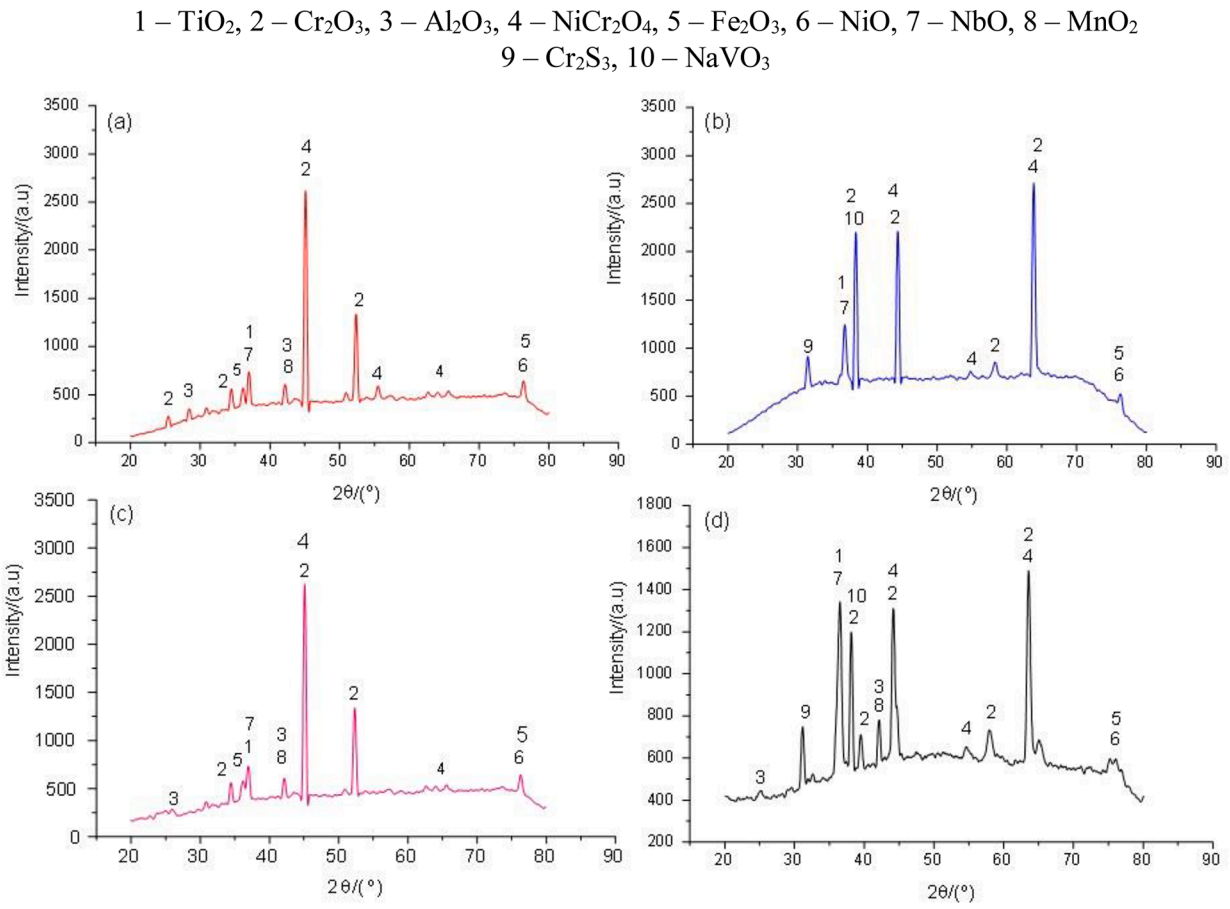


**Fig. 7.** XRD analysis of alloy 80A welded with ERNiCr-3 filler wire (a) GTAW- air oxidation (b) GTAW - molten salt; (c) PCGTAW - air oxidation and (d) PCGTAW - molten salt.

**Table 3**
Prominent and minor oxide phases of the welded substrate after exposure to the AO and MS environments at 900 °C.

| Sample | | Prominent phase | Minor Phases |
|---|---|---|---|
| ERNiCrMo-3 | GTAW – Air Oxidation | $Cr_2O_3$, $TiO_2$ | $Al_2O_3$, $MoO_3$, NbO, $MnO_2$, $NiCr_2O_4$, NiO, $Fe_2O_3$ |
| | GTAW – Molten salt | $Cr_2O_3$, $TiO_2$, $MoO_3$, $NiCr_2O_4$, NbO, $NaVO_3$ | $Al_2O_3$, $MnO_2$, NiO, $Fe_2O_3$, $Cr_2S_3$ |
| | PCGTAW – Air Oxidation | $Cr_2O_3$ | $Al_2O_3$, $MoO_3$, NbO, $MnO_2$, $NiCr_2O_4$, NiO, $Fe_2O_3$, $MoO_3$ |
| | PCGTAW – Molten salt | $Cr_2O_3$, $TiO_2$, $MoO_3$, $NiCr_2O_4$, NbO, $NaVO_3$ | $Al_2O_3$, $MnO_2$, NiO, $Fe_2O_3$, $Cr_2S_3$ |
| ERNiCr-3 | GTAW – Air Oxidation | $Cr_2O_3$, $NiCr_2O_4$, NbO | $Al_2O_3$, $TiO_2$, $MnO_2$, NiO, $Fe_2O_3$ |
| | GTAW – Molten salt | $Cr_2O_3$, $NiCr_2O_4$, $NaVO_3$, NbO | $TiO_2$, NiO, $Fe_2O_3$, $Cr_2S_3$ |
| | PCGTAW – Air Oxidation | $Cr_2O_3$, $NiCr_2O_4$, NbO | $Al_2O_3$, $TiO_2$, $MnO_2$, NiO, $Fe_2O_3$ |
| | PCGTAW – Molten salt | $Cr_2O_3$, $NiCr_2O_4$, $NaVO_3$, $TiO_2$, NbO | $Al_2O_3$, $MnO_2$, NiO, $Fe_2O_3$, $Cr_2S_3$ |

3 substrate due to the protective $NiCr_2O_4$, NbO and $Cr_2O_3$ oxides and the absence of non-protective Mo element $MoO_3$ oxide in the substrate. PCGTAW Mo-3 substrate showed significant weight gain than GTAW Cr-3 substrate due to $MoO_3$ and $Fe_2O_3$ oxides on the substrate surface. Even though grain refinement results in more protective oxides, some Mo and Fe element diffusion is possible. The presence of Mo and Fe elements may have induced strain on the scale because $MoO_3$ oxides cause acidic fluxing on the alloy, which results in cracking, spallation and exfoliation of oxide scales. These cracks may allow the corrosive MS content to react with the sub-surface of the substrate, resulting in more weight gain [29]. A similar observation has been observed in the visual observation on PCGTAW Mo-3 substrate compared to GTAW Cr-3 substrate. $Fe_2O_3$ oxide presence is also observed in the XRD results of the PCGTAW Mo-3 substrate. In GTAW Mo-3 substrate, higher weight gain is observed due to an absence of grain refinement that forms less protective agents and the presence of $MoO_3$ and $Fe_2O_3$ oxides that accelerated the oxidation as more spallation in the substrate compared to other substrates.

The presence of $Cr_2S_3$ increases the weight gain of MS substrate. When Cr reacts with $Na_2SO_4$, it forms both sulfides and oxides, and these $Cr_2S_3$ are often seen in grain boundaries [30]. Kameswari [31] observed similar findings and stated that chromium sulfide oxidation is one of the key processes that drastically attacks the alloy and increases the weight. These $Cr_2S_3$ sulfides are oxidized to form $Cr_2O_3$.

$$Cr_2S_3 + \frac{3}{2}\,O_2 \rightarrow Cr_2O_3 + 3\,S \qquad (6)$$

[31]

The existence of the Mn as $MnO_2$ is observed on the top surface of the oxide layer. Sidhu et al. [19] stated that the Mn element diffuses from the substrate to the top surface layer of the oxide scales. Liu [32] also stated the presence of MnO or $MnCr_2O_4$ oxide as a white spot on the top surface of the substrate.

## Conclusions

High-performance materials such as alloy 80A were used for manufacturing the gas turbine component or heat exchangers. However, these components tend to deteriorate when exposed to harsh environmental conditions such as Na2SO4, V2O5, NaCl, etc. In this work, alloy 80 weldments are fabricated through GTAW and PCGTAW techniques using ERNiCrMo-3 and ERNiCr-3 filler wires. These weldments are then exposed to AO and MS ($Na_2SO_4 + 60\%V_2O_5$) environmental conditions at 900 °C, and their performance was discussed as follows:

1 MS environment substrates show more weight growth than AO substrates. MS-induced and accelerated the corrosion of the welded substrate.
2 PCGTAW substrates showed better performance/corrosion resistance than their respective GTAW substrate. Particularly PCGTAW Cr-3 substrate showed less weight gain due to grain refinement and protective NiO, $Cr_2O_3$, NbO, $NiCr_2O_4$ oxides.
3 The grain refinement in PCGTAW WZ leads to more dislocation planar that offers routes for elements diffusion (such as Cr and Ni) from the sub-surface to the weld face. These Cr and Ni elements react with oxygen to form more protective oxides such as $Cr_2O_3$ and $NiCr_2O_4$ layers on the weld surface, thereby minimising the weight gain of the PCGTAW substrate.
4 GTAW and PCGTAW Cr-3 substrates showed better corrosion resistance than Mo-3 substrates due to NiO, $Cr_2O_3$, NbO, $NiCr_2O_4$ oxides, and the absence of $MoO_3$ oxide on the substrate's surface.
5 The production of NiO, $Cr_2O_3$, NbO oxides, and spinel $NiCr_2O_4$ oxide on the substrates surface offered high oxidation resistance by preventing oxygen from diffusing into the substrate's sub-surface layer.
6 The usage of the PCGTAW welding technique resulted in WZ grain refinement. The grain refinement promotes the formation of more protective oxide on the welded substrates' surface, resulting in lesser weight gain of PCGTAW substrate in AO and MS environments at 900 °C.

## Declaration of Competing Interest

The uploaded manuscript doesn't have any conflict of interest with industrial or academic or any other organization.

## Reference


[1] D. Brough, H. Jouhara, The aluminium industry: a review on state-of-the-art technologies, environmental impacts and possibilities for waste heat recovery, Int. J. Thermofluids 1–2 (2020), 100007.
[2] J.J. Fierro, A. Escudero-Atehortua, C. Nieto-Londoño, M. Giraldo, H. Jouhara, L. C. Wrobel, Evaluation of waste heat recovery technologies for the cement industry, Int. J. Thermofluids 7–8 (2020), 100040.
[3] B. Egilegor, H. Jouhara, J. Zuazua, F. Al-Mansour, K. Plesnik, L. Montorsi, L. Manzini, ETEKINA: analysis of the potential for waste heat recovery in three sectors: aluminium low pressure die casting, steel sector and ceramic tiles manufacturing sector, Int. J. Thermofluids 1–2 (2020), 100002.
[4] P.K. Pandis, S. Papaioannou, V. Siaperas, A. Terzopoulos, V.N. Stathopoulos, Evaluation of Zn- and Fe- rich organic coatings for corrosion protection and condensation performance on waste heat recovery surfaces, Int. J. Thermofluids 3–4 (2020), 100025.
[5] M. McLean, Nickel-based alloys: recent developments for the aero-gas turbine. High-Performance Materials in Aerospace, Springer, Dordrecht, 1995, pp. 135–154.
[6] R.K. Mishra, D.K. Srivastav, K. Srinivasan, V. Nandi, R.R. Bhat, Impact of foreign object damage on an aero gas turbine engine, J. Fail. Anal. Prev. 15 (1) (2015) 25–32.
[7] T.J. Carter, Common failures in gas turbine blades, Eng. Fail. Anal. 12 (2) (2005) 237–247.
[8] S. Rani, A.K. Agrawal, V. Rastogi, Failure analysis of a first stage IN738 gas turbine blade tip cracking in a thermal power plant, Case Stud, Eng. Fail. Anal. 8 (1) (2017) 1–10.
[9] N. Eliaz, G. Shemesh, R.M. Latanision, Hot corrosion in gas turbine components, Eng. Fail. Anal. 9 (1) (2002) 31–43.
[10] R.A. Rapp, Y.S. Zhang, Hot corrosion of materials: fundamental studies, Jom 46 (12) (1994) 47–55.
[11] VDM® Alloy 80 A, Material Data Sheet No. 4048, VDM Metals International GmbH, 2017. https://www.vdm-metals.com/fileadmin/user_upload/Downloads/Data_Sheets/Data_Sheet_VDM_Alloy_80_A.pdf.
[12] N. Swain, P. Kumar, G. Srinivas, S. Ravishankar, H.C. Barshilia, Mechanical micro-drilling of nimonic 80A superalloy using uncoated and TiAlN-coated micro drills, Mater. Manuf. Processes 32 (13) (2017) 1537–1546.
[13] S. Kiamehr, K.V. Dahl, M. Montgomery, M.A. Somers, KCl-induced high temperature corrosion of selected commercial alloys: part II: alumina and silica-formers, Mater. Corros. 67 (1) (2016) 26–38.
[14] V. Sreenivasulu, M. Manikandan, High-temperature corrosion behaviour of air plasma sprayed $Cr_3C_2$-25NiCr and NiCrMoNb powder coating on alloy 80A at 900°C, Surf. Coat. Technol. 337 (1) (2018) 250–259.
[15] Eßer K.H. Keienburg, B. Deblon, Refurbishing procedures for blades of large stationary gas turbines, Mater. Sci. Technol. 1 (8) (1985) 620–628, https://doi.org/10.1179/mst.1985.1.8.620.
[16] S.H. Cho, J.M. Hur, C.S. Seo, S.W. Park, High temperature corrosion of superalloys in a molten salt under an oxidizing atmosphere, J. Alloys Compd. 452 (1) (2008) 11–15.
[17] P. Subramani, M. Manikandan, Development of welding technique to suppress the microsegregation in the aerospace grade alloy 80A by conventional current pulsing technique, J. Manuf Processes 34 (1) (2018) 579–592.
[18] P. Subramani, M. Manikandan, Development of gas tungsten arc welding using current pulsing technique to preclude chromium carbide precipitation in aerospace-grade alloy 80A, Int. J. Miner. Metall. Mater. 26 (2) (2019) 210–221.
[19] T.S. Sidhu, S. Prakash, R.D. Agrawal, Hot corrosion studies of HVOF sprayed $Cr_3C_2$–NiCr and Ni–20Cr coatings on nickel-based superalloy at 900 °C, Surf. Coat. Technol. 201 (3–4) (2006) 792–800.
[20] H. Singh, D. Puri, S. Prakash, R. Maiti, Characterization of oxide scales to evaluate high temperature oxidation behavior of Ni–20Cr coated superalloys, Mater. Sci. Eng. A 464 (1–2) (2007) 110–116.
[21] Z. Tong, X. Ren, Y. Ren, F. Dai, Y. Ye, W. Zhou, L. Chen, Z. Ye, Effect of laser shock peening on microstructure and hot corrosion of TC11 alloy, Surf. Coat. Technol. 335 (1) (2018) 32–40.
[22] B. Somasundaram, R. Kadoli, M.R. Ramesh, Hot corrosion behaviour of HVOF sprayed ($Cr_3C_2$–35% NiCr)+ 5% Si coatings in the presence of $Na_2SO_4$–60% $V_2O_5$ at 700°C, Trans. Indian Inst. Met. 68 (2) (2015) 257–268, https://doi.org/10.1007/s12666-014-0453-0.
[23] K.S. Sreenivas, V.M. Radhakrishnan, Oxidation and hot corrosion behaviour of Nimonic-75 superalloy, Indian J. Eng. Mater. Sci. 5 (5) (1998) 295–301.
[24] M. Kaur, H. Singh, S. Prakash, High-temperature behavior of a high-velocity oxy-fuel sprayed $Cr_3C_2$-NiCr coating, Metall. Mater. Trans. A 43 (8) (2012) 2979–2993.
[25] S.T. Bluni, A.R. Mardar, Effects of thermal spray coating composition and microstructure on coating response and substrate protection at high temperatures, Corrosion 52 (3) (1996) 213–218.
[26] T.S. Sidhu, S. Prakash, R.D. Agrawal, Performance of high-velocity oxyfuel-sprayed coatings on an Fe-based superalloy in $Na_2SO_4$-60% $V_2O_5$ environment at 900°C part II: hot corrosion behavior of the coatings, J. Mater. Eng. Perform. 15 (1) (2006) 130–138.
[27] H. Choi, B. Yoon, H. Kim, C. Lee, Isothermal oxidation of air plasma spray NiCrAlY bond coatings, Surf. Coat. Technol. 150 (2–3) (2002) 297–308.
[28] I.A. Kvernes, P. Kofstad, The oxidation behavior of some Ni-Cr-Al alloys at high temperatures, Metall. Trans. 3 (6) (1972) 1511–1519.
[29] R. Bhatia, H. Singh, B.S. Sidhu, Hot corrosion studies of HVOF-sprayed coating on T-91 boiler tube steel at different operating temperatures, J. Mater. Eng. Perform. 23 (2) (2014) 493–505, https://doi.org/10.1007/s11665-013-0771-0.
[30] R. Viswanathan, High temperature corrosion of some gas turbine alloys, Corrosion 24 (11) (1968) 359–368.
[31] S. Kameswari, The application of DTA to hot corrosion studies of chromium and nickel powders and nimonic 80A, J. Therm. Anal. Calorim. 31 (4) (1986) 813–824.
[32] Y. Liu, Performance evaluation of several commercial alloys in a reducing environment, J. Power Sources 179 (1) (2008) 286–291.